

Are your MRI contrast agents cost-effective?

Learn more about generic Gadolinium-Based Contrast Agents.



FRESENIUS  
KABI

caring for life

**AJNR**

## Phosphaturic Mesenchymal Tumor

J.C. Benson, J.A. Trejo-Lopez, A.M. Nassiri, K. Eschbacher,  
M.J. Link, C.L. Driscoll, R.D. Tiegs, J. Sfeir and D.R.  
DeLone

*AJNR Am J Neuroradiol* 2022, 43 (6) 817-822

doi: <https://doi.org/10.3174/ajnr.A7513>

<http://www.ajnr.org/content/43/6/817>

This information is current as  
of April 17, 2024.

# Phosphaturic Mesenchymal Tumor

J.C. Benson, J.A. Trejo-Lopez, A.M. Nassiri, K. Eschbacher, M.J. Link, C.L. Driscoll, R.D. Tiegs, J. Sfeir, and D.R. DeLone

## ABSTRACT

Phosphaturic mesenchymal tumors (PMTs) are neoplasms associated with tumor-induced osteomalacia. Patients typically present with pathologic fractures in the setting of chronic hypophosphatemic hyperphosphaturic osteomalacia, as well as gradual muscle weakness, bone pain, and difficulty walking. Because of their rarity and nonspecific symptomatology, phosphaturic mesenchymal tumors often go undiagnosed for years. Even when discovered on imaging, the tumors can be diagnostically challenging for radiologists. Phosphaturic mesenchymal tumors often tend to be small and can be located nearly anywhere in the body, and, therefore, can mimic many other tumors. This case highlights the imaging and pathologic markers of a phosphaturic mesenchymal tumor, often found in a patient with tumor-induced osteomalacia.

**ABBREVIATIONS:** FGF23 = fibroblast growth factor 23; PMT = phosphaturic mesenchymal tumor; TIO = tumor-induced osteomalacia

The patient is a 57-year-old man who presented to our institution for evaluation with a 4-year history of recurrent insufficiency fractures involving his femurs and ribs, associated with considerable disability. His initial symptom was right-hip pain that failed to resolve with conservative treatment. An MR imaging at that time showed a left subtrochanteric insufficiency fracture. Two years later, after developing pain in both thighs, the patient was diagnosed with insufficiency fractures involving the subtrochanteric regions of both proximal femurs. At the time of presentation, a review of his laboratory records revealed chronic hypophosphatemia, with serum phosphorus levels ranging between 1.7 and 2.1 mg/dL during the preceding 4 years. His serum calcium and parathyroid hormone levels have been consistently within the normal range.

Given his history and laboratory abnormalities, the diagnosis of tumor-induced osteomalacia (TIO) was entertained. Confirmatory testing (Table) demonstrated hypophosphatemia due to renal phosphate wasting, as well as elevated fibroblast growth factor 23 (FGF23).

The patient did not have skeletal deformities or a family history of bone disorders, and his bone density readings were in the osteopenia range. He then underwent a PET gallium ( $^{68}\text{Ga}$ )

DOTATATE study to examine for a mesenchymal tumor, which is the usual source of the excess FGF23 production.

## Imaging

The  $^{68}\text{Ga}$  DOTATATE examination demonstrated a focal lesion in the petrous aspect of the left temporal bone (Fig 1), considered highly suspicious for the patient's culprit lesion. Dedicated imaging of the temporal bone was therefore performed.

On MR imaging, an avidly enhancing lesion was seen along the cochlear promontory in the middle ear, extending into the anterior hypotympanum along the course of the Eustachian tube (Fig 2). Anteriorly, the mass involved the skull base, encroaching on the foramen spinosum. Posteriorly, the mass closely approximated the geniculate ganglion of the facial nerve. When read in conjunction with the  $^{68}\text{Ga}$  DOTATATE examination, this was initially thought to represent a glomus tympanicum tumor with unusual anterior growth. A glomus faciale tumor growing from the geniculate ganglion, phosphaturic mesenchymal tumor (PMT), primary neuroendocrine carcinoma, or metastasis were also considered.

On a subsequent CT, the tumoral margins were not well-demarcated because the density of the mass matched that of the fluid within the adjacent middle ear and mastoid air cells. However, the CT scans did reveal the mass to be permeative with destruction of the adjacent skull base (Fig 3). In retrospect, the patient did note a long-standing history of left-sided hearing loss and ear fullness without drainage.

Received January 3, 2022; accepted after revision March 17.

From the Departments of Radiology (J.C.B., D.R.D.), Laboratory Medicine and Pathology (J.A.T.-L., K.E.), Otorhinolaryngology (A.M.N., C.L.D.), Neurosurgery (M.J.L.), and Endocrinology (R.D.T., J.S.), Mayo Clinic, Rochester, Minnesota.

Please address correspondence to John C. Benson, MD, 200 1st St SW, Department of Radiology, Mayo Clinic, Rochester, MN 55905; e-mail: benson.john3@mayo.edu

<http://dx.doi.org/10.3174/ajnr.A7513>

### Patient laboratory testing on presentation

Levels	Results	Reference Range
Total serum calcium	9.0	8.8–10.2 mg/dL
Albumin	4.4	3.5–5.0 g/dL
Phosphorus	1.5	2.5–4.5 mg/dL
Magnesium	2.1	1.7–2.3 mg/dL
Creatinine	0.97	0.74–1.35 mg/dL
Alkaline phosphatase	102	35–104 U/L
Parathyroid hormone	64	15–65 pg/mL
25 (hydroxyvitamin) Vitamin D	83	30–50 ng/mL
1, 25 (hydroxyvitamin) <sub>2</sub> Vitamin D	29	18–64 pg/mL
Intact <i>FGF23</i>	82	≤59 pg/mL
Tubular reabsorption of phosphate	62%	>85%

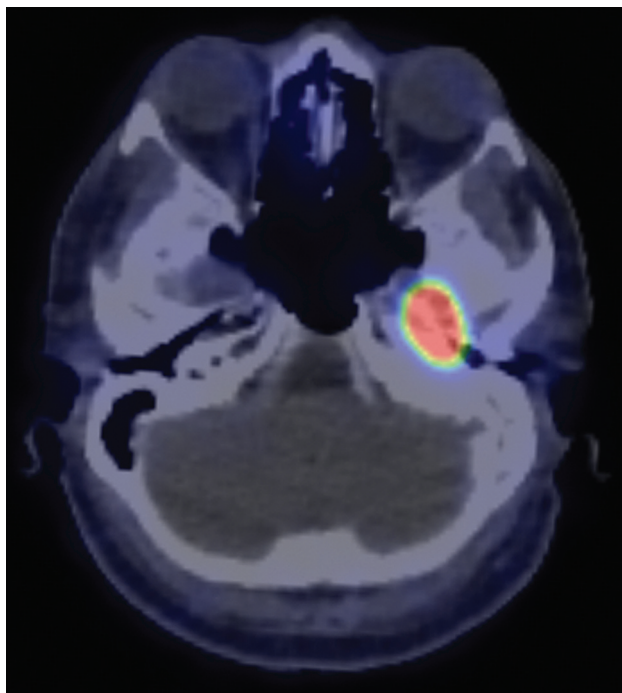


**FIG 1.** <sup>68</sup>Ga DOTATATE PET/CT demonstrates marked radiotracer uptake within the petrous aspect of the left temporal bone.

### Operative Report

On preoperative otoscopy, the mass was easily visible within the middle ear and less intensely red than a typical paraganglioma (which is typically deep red) (Fig 4). Considering the imaging findings and clinical history, the likely diagnosis was PMT, and surgical treatment was recommended. Tumoral resection was accomplished via a left middle cranial fossa craniotomy. Intraoperatively, the tumor was noted to have eroded through the middle fossa floor just posterior and lateral to foramen spinosum. No involvement of the subtemporal dura was noted intraoperatively, though this may have been due to the dural thickening noted on imaging being reactive in nature rather than tumoral extension. It appeared to originate at the anterior aspect of the Eustachian tube and extended along the Eustachian tube inferiorly into the middle ear. The tumor was quite vascular and required piecemeal excision with frequent use of hemostatic agents and bipolar cautery during resection. Angled instruments and otologic endoscopes were used to release the inferior extent of the tumor from the middle ear. Ultimately,

gross total resection was achieved. The patient had an uneventful postoperative course without signs of CSF leak or cranial nerve deficits.

### Pathology

Histologic examination of the tumor revealed a highly vascular neoplasm composed of predominantly spindled tumor cells with bland, ovoid nuclei with interspersed staghorn-like vessels (Fig 5). There were scattered coarse, flocculent calcifications. Neoplastic cells showed overall monotonous nuclei, with low proliferative activity and no tumor necrosis. Immunohistochemical studies revealed tumor cells to be diffusely positive for *SSTR2A*, while negative for chromogranin and synaptophysin. In addition, there was widespread expression by the tumor cells of *FGF23* mRNA by chromogenic in situ hybridization. Overall, these findings supported the final diagnosis of a morphologically benign PMT.

Histologically, PMTs are highly vascular and composed of bland, spindled-to-stellate cells in a distinctive myxoid or myxochondroid matrix with flocculent calcification.<sup>1–3</sup> *FNI-FGFRI* or *FNI-FGF1* fusions are common in PMTs (up to approximately 50%), which may activate the *FGFR1* pathway leading to increased expression of the *FGF23* gene and protein.<sup>1–3</sup> *FGF23* expression can be detected by reverse-transcription polymerase chain reaction, chromogenic in situ hybridization, or immunohistochemistry.<sup>1,2</sup>

The histologic differential diagnosis of this tumor includes solitary fibrous tumor, mesenchymal chondrosarcoma, and paraganglioma. Solitary fibrous tumors can have staghorn vessels and have a similar, bland, spindle cell appearance. However, solitary fibrous tumors lack the characteristic matrix and calcifications of PMTs and would not express *SSTR2A* or *FGF23* mRNA.<sup>2,3</sup> Mesenchymal chondrosarcomas have malignant, small, round cells; lack the characteristic calcified matrix of a PMT; and would not express *FGF23* mRNA. A highly vascular paraganglioma may, at times, be morphologically reminiscent of PMT. However, the immunophenotype of PMT (positive for *SSTR2A* and *FGF23* mRNA, negative for chromogranin and synaptophysin) excluded this possibility. Furthermore, although paragangliomas and PMTs can both exhibit high vascularity, paragangliomas lack the characteristic chondromyxoid matrix and calcifications of PMT. Unlike PMTs, paragangliomas have a characteristic nested (zellballen) architecture composed of neuroendocrine cells and are positive for neuroendocrine markers (eg, synaptophysin and chromogranin). The tumor presented here did not have the classic morphology of paraganglioma and was negative for synaptophysin and chromogranin.

### DISCUSSION

PMTs are exceedingly rare tumors that arise primarily from bones and connective tissue. They are typically seen in middle-aged adults without an apparent sex predilection. Pediatric cases have been infrequently reported.<sup>4</sup> The median age at the time of diagnosis is 44–48 years of age.<sup>5,6</sup> Tumor locality is unpredictable; PMTs can be found in any osseous or soft-tissue location and uncommonly involve the skin.<sup>7</sup> More than half of the tumors are found within the extremities, with the femur being the most common site.<sup>8</sup> Within the head and neck, the sinonasal region is most common, followed by the mandible and maxilla. Although histologically benign, rare cases of malignant transformation and metastases have been reported.<sup>8–10</sup>

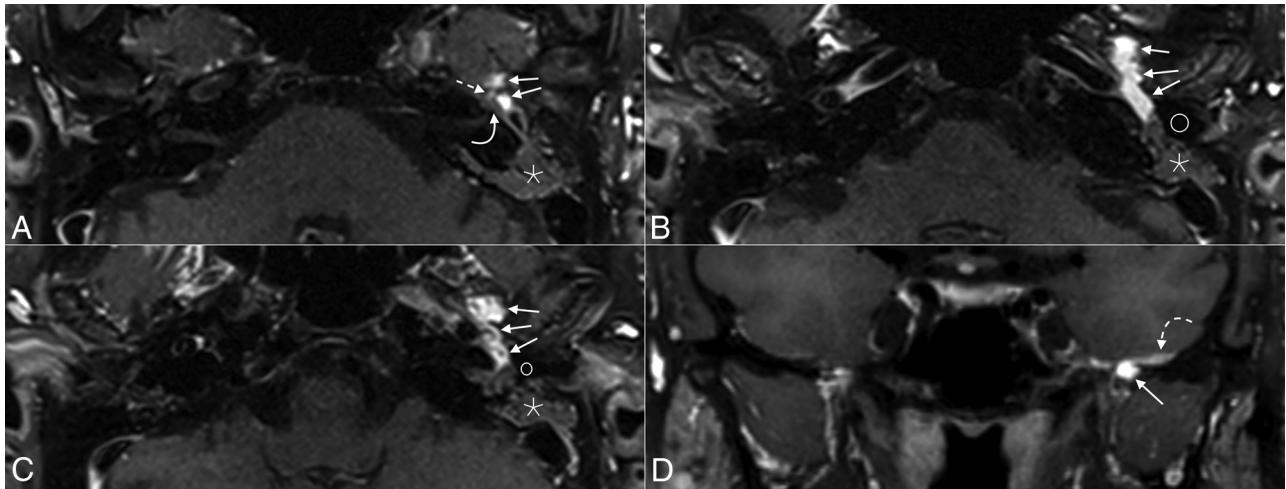


**FIG 2.** From superior to inferior, axial (A–C) MR images show an avidly enhancing mass (solid arrows) extending from the middle ear along the floor of the middle cranial fossa, with substantial intraosseous involvement. A small portion of the mass (dashed straight arrow) closely approximates the geniculate ganglion of the facial nerve (solid curved arrow) (circles in B and C denote the external auditory canal). The mastoid air cells are completely opacified (asterisks). Coronal image (D) shows the mass extending intracranially, with associated dural thickening (dashed curved arrow).

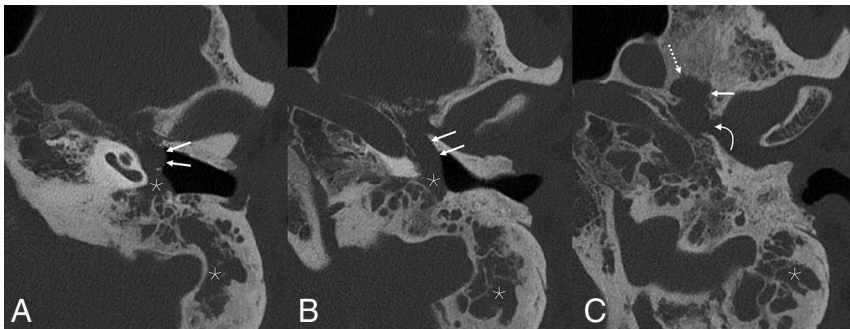


**FIG 3.** Noncontrast temporal bone CT performed 2 days after MR imaging again shows the mass (solid straight arrows) extending from the mesotympanum (A) into the anterior hypotympanum (B), which is widened. The mass is locally destructive (C), causing erosion of the skull base with involvement of the foramen spinosum (dashed straight arrow) and left temporomandibular joint (curved arrow). The margins of the mass are indistinguishable from fluid density within the middle ear and mastoid air cells (asterisks), which remained opacified.

Clinically, PMTs are associated with tumor-induced osteomalacia (TIO), also known as oncogenic osteomalacia, a paraneoplastic syndrome characterized by widespread reduction of osteoblastic activity. PMTs secrete FGF23, a peptide hormone-like regulator of phosphate levels, which decreases re-absorption of phosphate in the proximal tubules of the kidneys, causing it to be wasted within the urine. The downstream suppression of osteoblasts and mobilization of calcium and phosphate from the bones lead to widespread hypophosphatemic osteomalacia.<sup>11</sup> Patients present with bone pain, insufficiency fractures, and gradual-onset muscular weakness.<sup>12</sup>

A rare subtype of PMT has recently been identified as being nonphosphaturic.<sup>13</sup> The descriptions of these tumors are heterogeneous. Some might produce negligible amounts of FGF23 or are thought to exist in patients with a compensatory mechanism in place.<sup>3</sup> Some are thought to produce a deformed and/or inactive form of the FGF23 protein.<sup>14</sup> Other tumors may

simply have been identified in patients before symptomatic osteomalacia had developed.<sup>15</sup>

Unfortunately, the rarity of PMTs makes them notoriously under-recognized by clinicians. Many patients are symptomatic for years or decades before the tumor is diagnosed.<sup>16,17</sup> The diagnosis typically is based on a combination of clinical history, laboratory values, and imaging. Specifically, elevated serum FGF23 levels in a patient with hypophosphatemia and normal renal function is highly suggestive of a PMT. However, TIO has a known association with multiple other tumors, typically of mesenchymal origin, including solitary fibrous tumors, giant cell tumors, chondrosarcomas, and osteosarcomas.<sup>18,19</sup>

Most, but not all, of these tumors result in TIO through the secretion of FGF23; some secrete various other factors such as frizzled-related protein-4, *FGF7*, and matrix extracellular phosphoglycoprotein.<sup>20</sup>

Once the diagnosis of TIO has been established, various nuclear medicine studies can be used to search for the culprit lesion, including <sup>68</sup>Ga DOTATATE, technetium Tc99m-octreotide, and FDG PET/CT scans.<sup>21</sup> <sup>68</sup>Ga DOTATATE is now the favored technique, having been shown to have the greatest sensitivity for tumoral detection.<sup>15, 22–24</sup> This superiority of <sup>68</sup>Ga DOTATATE over other modalities is thought to be due to the higher affinity of its radiotracer to somatostatin receptors 2 and 5, which are expressed by PMTs.<sup>23</sup> Nevertheless, the sensitivity of these examinations is suboptimal. A series by El-Maouche et al<sup>23</sup> found that <sup>68</sup>Ga DOTATATE examinations found a PMT in just more than half of patients with hypophosphatemic TIO, while indium-111





**FIG 4.** Preoperative otoscopy of the left tympanic membrane reveals a reddish mass (*arrowheads*) within the anterior mesotympanum. An amber effusion (*star*) is seen posterior to the mass, surrounding the incudostapedial joint (*asterisk*).

(<sup>111</sup>In) pentetreotide (OctreoScan) SPECT/CT and [<sup>18</sup>F] FDG identified <50%.

PMTs are not encapsulated and tend to be locally infiltrative.<sup>12</sup> On CT, intraosseous PMTs are osteolytic with a narrow zone of transition and internal matrix; soft-tissue masses are hypodense and enhance.<sup>25</sup> On MR imaging, tumors are isointense to soft tissues on T1-weighted imaging and demonstrate enhancement.<sup>26</sup> Intralesional T2 signal is variable. Most commonly, tumors are T2-hyperintense, though Broski et al<sup>22</sup> noted that PMTs characteristically have small foci of intralesional T2 hypointensity. Some may be partially cystic. Larger tumors may have intralesional flow voids.<sup>27</sup> However, most PMTs are small and slow-growing, and tumor localization is highly variable. Thus, they may present a diagnostic conundrum for radiologists, particularly when the diagnosis of TIO is unknown, or, as in this case, if the PMT mimics the appearance of a more common entity.<sup>26</sup>

The only known definitive treatment for TIO is surgical resection of the tumor. Fortunately, removal of PMTs results in complete resolution of the biochemical and physical sequelae of the paraneoplastic syndrome.<sup>7</sup> Because PMTs are often locally invasive, a wide excision is needed to successfully obtain tumor-free margins.<sup>28</sup> Although local recurrence may occur, surgical resection is considered curative in approximately 90% of cases.<sup>27,29</sup> Cryoablation has been successfully used to treat residual tumor after resection.<sup>30</sup> For patients with unresectable tumors, a fully human monoclonal antibody against FGF23, burosumab, has

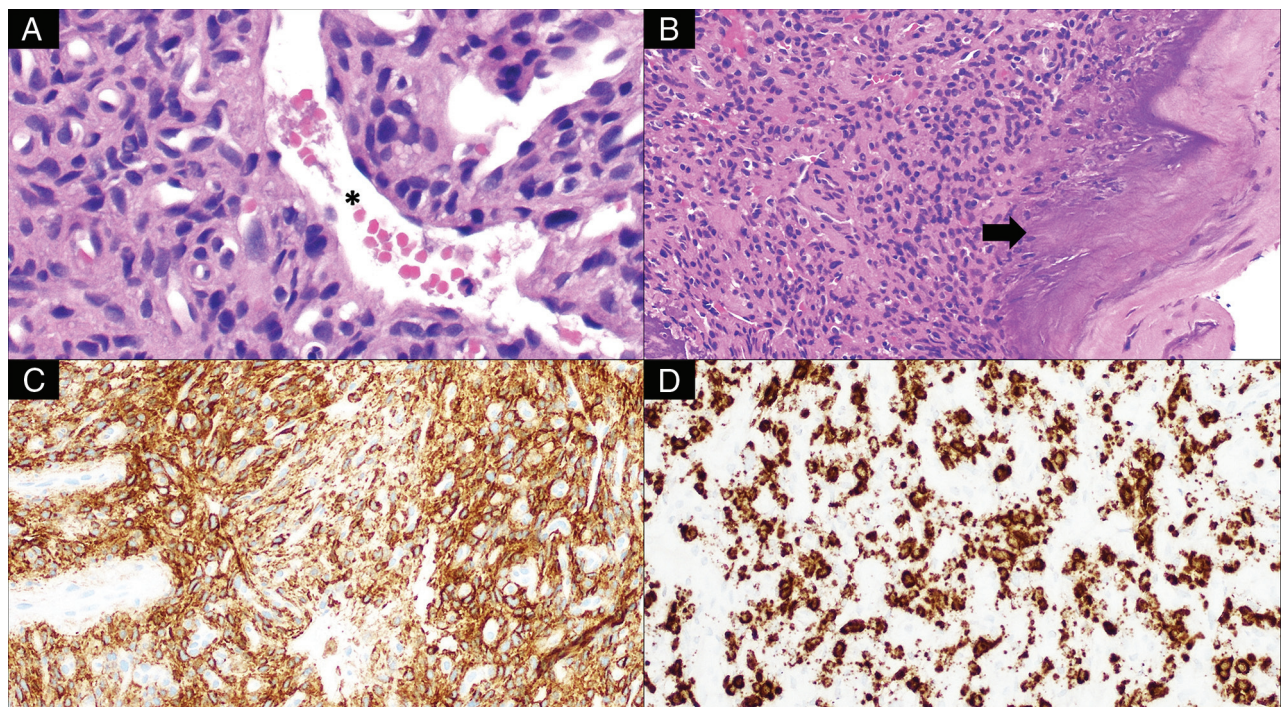


**FIG 5.** Histologic examination of this tumor reveals bland, spindled-to-stellate neoplastic cells (A, H&E, original magnification  $\times 400$ ) situated in a hyalinized matrix with a well-developed capillary network including ectatic, staghorn vessels (*asterisk*) as well as characteristic deposition of coarse calcification (B, H&E, original magnification  $\times 200$ ; *arrow*). The tumor is reactive for *SSTR2A* (C, immunohistochemistry, original magnification  $\times 200$ ) and shows evidence of *FGF23* mRNA expression (D, chromogenic in situ hybridization, original magnification  $\times 200$ ).

been shown to provide biochemical and symptomatic improvement and was recently FDA-approved.<sup>31</sup>

Difficult cases are excellent learning opportunities, and this case is no exception. Despite the difficulty of the resection, the surgeons indicated that the available preoperative imaging was excellent, and they stated that additional imaging would not have changed the surgical approach. In retrospect, the differential considerations given in the initial radiology report could have been more precise. The case was challenging due to its location in an anatomic region that can support the growth of paragangliomas. Nevertheless, the clinical history of TIO should have served as a more convincing indicator that the tumor identified on imaging represented a PMT. Incorrectly favoring a paraganglioma over a PMT could have delayed or even prevented surgery because the purpose of the examination was to search for a lesion responsible for the patient's TIO. Fortunately, the patient ultimately underwent the best treatment course. He is expected to make a full recovery and will undergo routine surveillance imaging to monitor for recurrence.

### Case Summary

- PMTs are extremely rare entities that are associated with TIO.
- The tumors are small and can be found nearly anywhere in the body, making them a common mimic of more common malignancies.
- Surgical resection of the tumor results in resolution of a patient's osteomalacia.
- Histologically, PMTs have an unusual, hyalinized matrix that undergoes calcification with frequent expression of *FGF23* mRNA.

Disclosure forms provided by the authors are available with the full text and PDF of this article at [www.ajnr.org](http://www.ajnr.org).

### REFERENCES

1. Lee J, Folpe AL. Phosphaturic mesenchymal tumor. In: Editorial Board. *WHO Classification of Tumours: Soft Tissue and Bone Tumours*. International Agency for Research on Cancer; 2020
2. Bahrami A, Weiss SW, Montgomery E, et al. **RT-PCR analysis for FGF23 using paraffin sections in the diagnosis of phosphaturic mesenchymal tumors with and without known tumor-induced osteomalacia.** *Am J Surg Pathol* 2009;33:1348–54 [CrossRef Medline](#)
3. Folpe AL, Fanburg-Smith JC, Billings SD, et al. **Most osteomalacia-associated mesenchymal tumors are a single histopathologic entity: an analysis of 32 cases and a comprehensive review of the literature.** *Am J Surg Pathol* 2004;28:1–30 [CrossRef Medline](#)
4. Kumar S, Shah R, Patil V, et al. **Tumor-induced rickets-osteomalacia: an enigma.** *J Pediatr Endocrinol Metab* 2020 July 20. [Epub ahead of print] [CrossRef Medline](#)
5. Honda R, Kawabata Y, Ito S, et al. **Phosphaturic mesenchymal tumor, mixed connective tissue type, non-phosphaturic variant: report of a case and review of 32 cases from the Japanese published work.** *J Dermatol* 2014;41:845–49 [CrossRef Medline](#)
6. Wu H, Bui MM, Zhou L, et al. **Phosphaturic mesenchymal tumor with an admixture of epithelial and mesenchymal elements in the jaws: clinicopathological and immunohistochemical analysis of 22 cases with literature review.** *Mod Pathol* 2019;32:189–204 [CrossRef Medline](#)
7. Hodgson SF, Clarke BL, Tebben PJ, et al. **Oncogenic osteomalacia: localization of underlying peripheral mesenchymal tumors with use of Tc 99m sestamibi scintigraphy.** *Endocr Pract* 2006;12:35–42 [CrossRef Medline](#)
8. Oyama N, Kojima-Ishii K, Toda N, et al. **Malignant transformation of phosphaturic mesenchymal tumor: a case report and literature review.** *Clin Pediatr Endocrinol* 2020;29:69–75 [CrossRef Medline](#)
9. Morimoto T, Takenaka S, Hashimoto N, et al. **Malignant phosphaturic mesenchymal tumor of the pelvis: a report of two cases.** *Oncol Lett* 2014;8:67–71 [CrossRef Medline](#)
10. Qiu S, Cao LL, Qiu Y, et al. **Malignant phosphaturic mesenchymal tumor with pulmonary metastasis: a case report.** *Medicine (Baltimore)* 2017;96:e6750 [CrossRef Medline](#)
11. Ghorbani-Aghbolaghi A, Darrow MA, Wang T. **Phosphaturic mesenchymal tumor (PMT): exceptionally rare disease, yet crucial not to miss.** *Autops Case Rep* 2017;7:32–37 [CrossRef Medline](#)
12. Pelo S, Gasparini G, Garagiola U, et al. **Phosphaturic mesenchymal tumor, an unusual localization in head and neck.** *J Surg Case Rep* 2018;2018:rjy091 [CrossRef Medline](#)
13. Shiba E, Matsuyama A, Shibuya R, et al. **Immunohistochemical and molecular detection of the expression of FGF23 in phosphaturic mesenchymal tumors including the non-phosphaturic variant.** *Diagn Pathol* 2016;11:26 [CrossRef Medline](#)
14. Winters R, Bihlmeyer S, McCahill L, et al. **Phosphaturic mesenchymal tumour-mixed connective tissue variant without oncogenic osteomalacia.** *J Clin Pathol* 2009;62:760–61 [CrossRef Medline](#)
15. Folpe AL. **Phosphaturic mesenchymal tumors: a review and update.** *Semin Diagn Pathol* 2019;36:260–68 [CrossRef Medline](#)
16. Adnan Z, Nikomarov D, Weiler-Sagie M, et al. **N. Phosphaturic mesenchymal tumors among elderly patients: a case report and review of literature.** *Endocrinol Diabetes Metab Case Rep* 2019;2019:18–139 [CrossRef Medline](#)
17. Drezner MK. **Tumor-induced osteomalacia.** *Rev Endocr Metab Disord* 2001;2:175–86 [CrossRef Medline](#)
18. Cho SI, Do NY, Yu SW, et al. **Nasal hemangiopericytoma causing oncogenic osteomalacia.** *Clin Exp Otorhinolaryngol* 2012;5:173–76 [CrossRef Medline](#)
19. Edmister KA, Sundaram M. **Oncogenic osteomalacia.** *Semin Musculoskelet Radiol* 2002;6:191–96 [CrossRef Medline](#)
20. Jagtap VS, Sarathi V, Lila AR, et al. **Tumor-induced osteomalacia: a single center experience.** *Endocr Pract* 2011;17:177–84 [CrossRef Medline](#)
21. Liu S, Zhou X, Song A, et al. **Successful treatment of tumor-induced osteomalacia causing by phosphaturic mesenchymal tumor of the foot.** *Medicine (Baltimore)* 2019;98:e16296 [CrossRef Medline](#)
22. Broski SM, Folpe AL, Wenger DE. **Imaging features of phosphaturic mesenchymal tumors.** *Skeletal Radiol* 2019;48:119–27 [CrossRef Medline](#)
23. El-Maouche D, Sadowski SM, Papadakis GZ, et al. **<sup>68</sup>Ga-DOTATATE for tumor localization in tumor-induced osteomalacia.** *J Clin Endocrinol Metab* 2016;101:3575–81 [CrossRef Medline](#)
24. Ha S, Park S, Kim H, et al. **Successful localization using <sup>68</sup>Ga-DOTATOC PET/CT of a phosphaturic mesenchymal tumor causing osteomalacia in a patient with concurrent follicular lymphoma.** *Nucl Med Mol Imaging* 2018;52:462–67 [CrossRef Medline](#)
25. Kawthalkar AS, Janu AK, Deshpande MS, et al. **Phosphaturic mesenchymal tumors from head to toe: imaging findings and role of the radiologist in diagnosing tumor-induced osteomalacia.** *Indian J Orthop* 2020;54:215–23 [CrossRef Medline](#)
26. Walsh EM, Jacob J, Lucas DR, et al. **Phosphaturic mesenchymal tumor of the cerebellopontine angle.** *JAMA Otolaryngol Head Neck Surg* 2019;145:287–88 [CrossRef Medline](#)
27. Richardson AL, Richardson OK. **Phosphaturic mesenchymal tumor: case report.** *Radiol Case Rep* 2019;14:1518–24 [CrossRef Medline](#)



28. Kane SV, Kakkar A, Oza N, et al. **Phosphaturic mesenchymal tumor of the nasal cavity and paranasal sinuses: a clinical curiosity presenting a diagnostic challenge.** *Auris Nasus Larynx* 2018;45:377–83 [CrossRef Medline](#)
29. Radaideh AR, Jaradat D, Abu-Kalaf MM, et al. **Resolution of severe oncogenic hypophosphatemic osteomalacia after resection of a deeply located soft-tissue tumour.** *Curr Oncol* 2009;16:87–90 [CrossRef Medline](#)
30. Horng JC, Van Eperen E, Tutton S, et al. **Persistent phosphaturic mesenchymal tumor causing tumor-induced osteomalacia treated with image-guided ablation.** *Osteoporos Int J Int* 2021;32:1895–98 [CrossRef Medline](#)
31. Brandi ML, Clunie GP, Houillier P, et al. **Challenges in the management of tumor-induced osteomalacia (TIO).** *Bone* 2021;152:116064 [CrossRef Medline](#)